

Topically applied Chitosan-Coated Poly(isobutylcyanoacrylate) Nanoparticles are Active Against Cutaneous Leishmaniasis by Accelerating Lesion Healing and Reducing the Parasitic Load

Sophia Malli ^{1,2}, Sebastien Pomel ², Yasmine Ayadi ^{1,2}, Claudine Deloménie ³, Antonio Da Costa ⁴,
Philippe M. Loiseau ², Kawthar Bouchemal ^{5*}

1. Institut Galien Paris Sud, UMR CNRS 8612, Univ. Paris-Sud, Université Paris-Saclay, Faculté de Pharmacie, 5, rue J-B. Clément, 92296, Châtenay-Malabry, France
2. BioCIS « Biomolécules : Conception, Isolement, Synthèse » - « Chimiothérapie Antiparasitaire », UMR CNRS 8076, Univ. Paris-Sud, Université Paris-Saclay, Faculté de Pharmacie, 5, rue J.B. Clément, 92296 Châtenay-Malabry cedex, France
3. Faculté de Pharmacie, Institut Paris Saclay d'Innovation Thérapeutique, UMS Inserm CNRS UPSud, Université Paris-Saclay, Châtenay-Malabry cedex, France
4. Université d'Artois, CNRS, Centrale Lille, ENSCL, Université Lille, UMR 8181, Unité de Catalyse et de Chimie du Solide (UCCS), Faculté Jean-Perrin, Rue Jean Souvras – SP 18, 62307 Lens, France
5. Institut Galien Paris Sud, Junior member of the Institut Universitaire de France, UMR CNRS 8612, Univ. Paris-Sud, Université Paris-Saclay, Faculté de Pharmacie, 5, rue J-B. Clément, 92296, Châtenay-Malabry, France

*Corresponding author: kawthar.bouchemal@u-psud.fr

Table of Contents

I. NP formulation and characterization	S-3
II. <i>In vitro</i> antileishmanial activity evaluation	S-4
II.1. Cultures of <i>Leishmania major</i> promastigotes and axenic amastigotes	S-4
II.2. <i>In vitro</i> evaluation in promastigotes	S-4
II.3. <i>In vitro</i> evaluation in axenic amastigotes	S-5
II.4. <i>In vitro</i> evaluation in intramacrophage amastigotes	S-5
III. Histological examinations of mouse skin	S-6
III.1. Healthy non-infected mouse skin	S-6
III.2. Infected and nontreated mouse skin	S-7
III.3. Mice treated by IL injections of AmB-DOC	S-8
III.4. Mice treated by IL injections of Cs-NPs	S-9
III.5. Mice treated by IL injections of the combination of AmB-DOC and Cs-NPs	S-10
III.6. Mice treated with topical application of F127 hydrogel	S-11
III.7. Mice treated topically with AmB-DOC _{F127}	S-12
III.8. Mice treated topically with Cs-NPs _{F127}	S-13
III.9. Mice treated with the combination (Cs-NPs/AmB-DOC) _{F127}	S-14
IV. Quantification of mice actin by q-PCR	S-15
IV.1. Genomic DNA preparation	S-15
IV.2. q-PCR analysis	S-15
IV.3. Results of the quantification of mice actin by q-PCR	S-16
V. TEM observations	S-17
V.1. Experimental method for the investigation of the <i>L. major</i> ultrastructure after incubation with Cs-NPs using TEM	S-17
V.2. TEM image of control untreated sample	S-17
V.3. TEM image after 20-min incubation with Cs-NPs	S-18
V.4. TEM image after 1-h incubation with Cs-NPs	S-19
References	S-19

IV. Nanoparticle formulation and characterization

Nanoparticles were formulated as previously reported in our research works.¹⁻² Briefly, 0.069 g of chitosan (Average molecular weight was 20,000 g/mol according to the manufacturer, Amicogen, Seoul, Korea) or 0.100 g of Pluronic® F68 (Poloxamer P188, BASF ChemTrade GmbH, Ludwigshafen, Germany) were dissolved in 5 mL of 0.2 M nitric acid (Acros Chemicals, Thermo Fisher Scientific, Geel, Belgium) in a glass tube at 40°C under vigorous magnetic stirring and argon bubbling. After 10 min, 0.25 mL of isobutylcyanoacrylate monomer (IBCA, Henkel Biomedical, Dublin, Ireland) were added. Argon bubbling was kept for additional 10 min and stopped. The reaction was allowed to continue at 40°C under vigorous magnetic stirring for 24 h. The pH of NP suspensions was adjusted to 4.5 by NaOH 0.1 N and stored at 4°C until use. Chitosan-coated nanoparticles are denoted Cs-NPs. Nanoparticles without chitosan stabilized by F68 are denoted F68-NPs. The mean hydrodynamic diameter of NPs and their size distribution were determined from the Z-average obtained at 20°C by quasi-elastic light scattering using Zetasizer Nanoseries (Malvern Instruments Ltd. UK). The scattered angle was fixed at 173° and 60 µL of each sample was diluted in 2 mL of MilliQ® water (Millex, SLAP 0225, Millipore, France). Zeta potential of NPs was measured using Zetasizer Nanoseries (Malvern Instruments Ltd. UK). The dilution of the suspensions (1:33 (v/v)) was performed in NaCl (1 mM). Each experiment was conducted in triplicate.

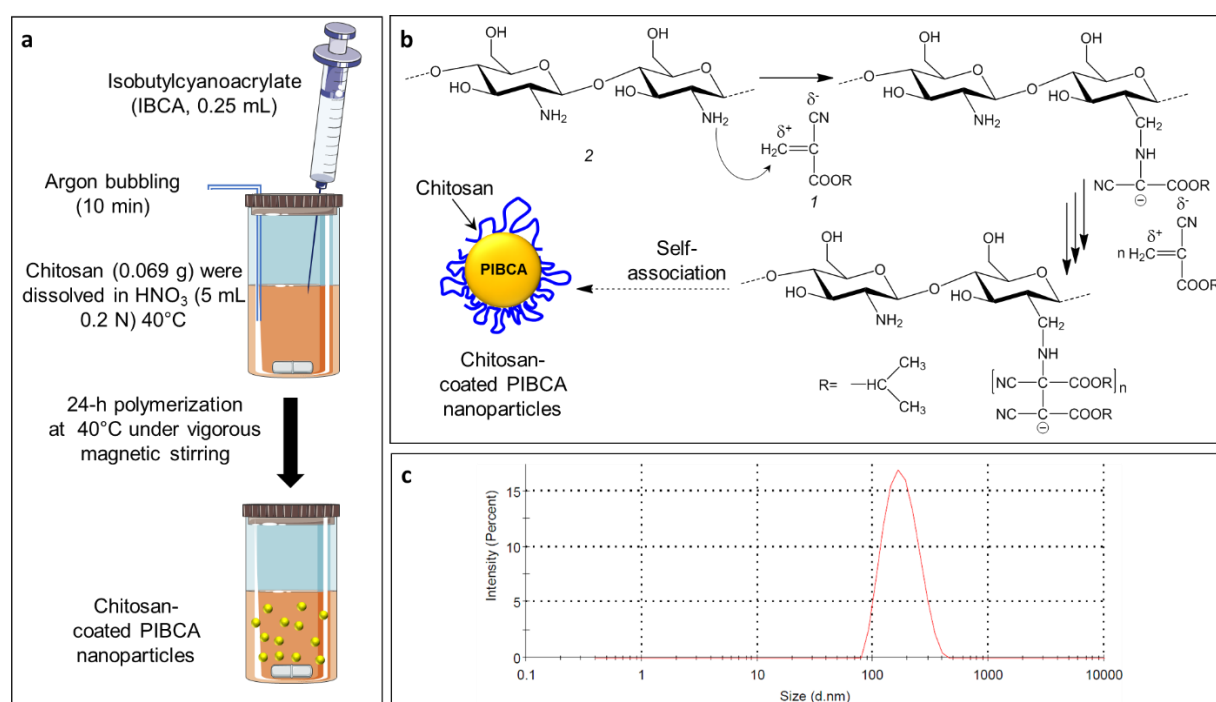


Figure S1. (a) Schematic representation of the general procedure for the formulation of chitosan-coated poly(isobutylcyanoacrylate) (PIBCA) nanoparticles. (b) The polymerization of isobutylcyanoacrylate monomer on the amine groups of deacetylated units of chitosan (2) according to anionic mechanism. (c) Size distribution of PIBCA nanoparticles coated with chitosan obtained by quasi-elastic light scattering analysis.

Nanoscale measurements were performed by atomic force microscopy (AFM) using a commercial microscope (Asylum Research/Oxford Instruments, MFP-3D) working in air at room temperature. The images were recorded in noncontact mode, where, the cantilever oscillates near the surface of the sample without contact. The images were obtained with silicon tip, drive frequency of 270 KHz and spring constant of 42 N/m. Cs-NP suspension was diluted in water (1/30) and 2 μ L were placed on freshly cleaved mica then 10 min-drying. The dry sample is deposited on freshly cleaved mica.

II. *In vitro* antileishmanial activity evaluation

II.1. Cultures of Leishmania major promastigotes and axenic amastigotes

L. major (MHOM/SU/73/5-ASKH/LEM134) promastigote culture was performed as previously reported by Daligaux et al.³ The temperature was fixed at 26°C and the samples were protected from light in M199 medium supplemented with NaHCO₃ (4.2 mM), heat-inactivated fetal bovine serum (10%), Hepes (40 mM at pH 7.5, 100 μ M) adenosine, 20 μ M Hemin (M199 complete medium), and 50 μ g/mL gentamycin.

Axenic amastigotes were cultured according to our previous works.⁴ Briefly, axenic amastigotes were obtained by incubating late log promastigotes 37°C with 5% CO₂ for 24 h in M199 complete medium acidified at pH 5.5.⁴ The experiments were performed with parasites in their logarithmic phase of growth.⁵

RAW 264.7 macrophages were maintained at 37°C with 5% CO₂ in DMEM supplemented with 10% heat-inactivated fetal bovine serum and 100 U/mL of penicillin-streptomycin (DMEM complete medium).

II.2. In vitro evaluation in promastigotes

Evaluation of formulations in promastigotes was performed as previously described⁶ with slight modifications. Briefly, two-fold serial dilutions of formulations were performed in 100 μ L in 96-well microplates in M199 complete medium. Exponentially growing promastigotes were then added to each well at 10⁶/mL in a 200- μ L final volume. After 72 h of incubation at 37°C with 5% CO₂, 20 μ L of resazurin at 450 μ M was added to each well, followed by further incubation in the dark for 24 h at 37°C. In living cells, resazurin is reduced in resorufin and this conversion is monitored by measuring OD_{570nm} (resorufin) and OD_{600nm} (resazurin; LabSystems Multiskan MS, LabSystem, Finland). The activity of the compounds was expressed as IC₅₀ in μ M (concentration of drug inhibited by 50% of the parasite growth compared with the controls treated with the excipient only).

II.3. In vitro evaluation in axenic amastigotes

Formulation activity in axenic and intramacrophage amastigotes was performed as previously described.^{4, 7} Two-fold serial dilutions of the formulations were performed in 100 μ L of the axenic

amastigote culture medium in 96-well microplates. Axenic amastigotes were then added to each well at 10^6 /mL in a 200- μ L final volume. After 72 h of incubation at 37°C with 5% CO₂, 20 μ L of 450 μ M resazurin was added to each well and was further incubated in the dark for 24 h at 37°C with 5% CO₂. In living cells, resazurin is reduced in resofurin. This conversion is monitored by measuring the absorbance at specific wavelengths of resofurin (570 nm) and resazurin (600 nm) using a microplate reader (LabSystems Multiskan MS). The antileishmanial activity of formulations was expressed as IC₅₀.

II.4. In vitro evaluation in intramacrophage amastigotes

For intramacrophage amastigotes, RAW 264.7 macrophages were plated in 96-well microplates at 2×10^4 cells per well and were incubated for 24 h at 37°C with 5% CO₂.⁶ Axenic amastigotes were induced as described above, centrifuged at 2000 rpm for 10 min, resuspended in DMEM complete medium, and added to each well at 3.2×10^5 parasites per well to reach a parasite to macrophage ratio of 16:1 as reported by Daligaux et al.³ After 24 h of infection at 37°C with 5% CO₂, extracellular parasites were removed and 100 μ L of DMEM complete medium containing two-fold serial dilutions of the formulations was added to each well. After 48 h of treatment, the medium was removed and replaced with 100 μ L of DirectPCR Lysis Reagent (Euromedex, Souffelweyersheim, France) before 3 freeze-thaw cycles at room temperature, the addition of 50 μ g/mL of proteinase K, and a final incubation at 55°C for 4 h to allow cell lysis. Next, 10 μ L of each cell extract was added to 40 μ L of DirectPCR Lysis reagent containing 0.05% Sybr Green I (Invitrogen, Saint-Aubin, France). DNA fluorescence was monitored using Mastercycler® realplex (Eppendorf, Montesson, France).³ The antileishmanial activity of formulations was expressed as IC₅₀.

III. Histological examinations of mouse skin

III.1. Healthy noninfected mouse skin

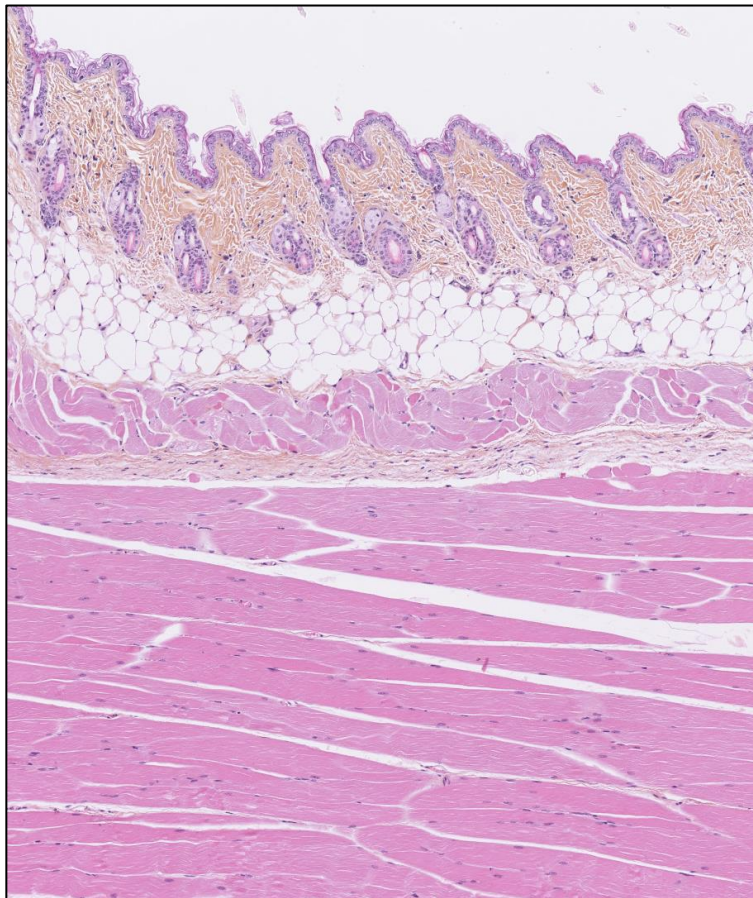


Figure S2: High magnification of high-resolution scan of a healthy mouse skin sample after HES staining.

III.2. Infected and nontreated mouse skin

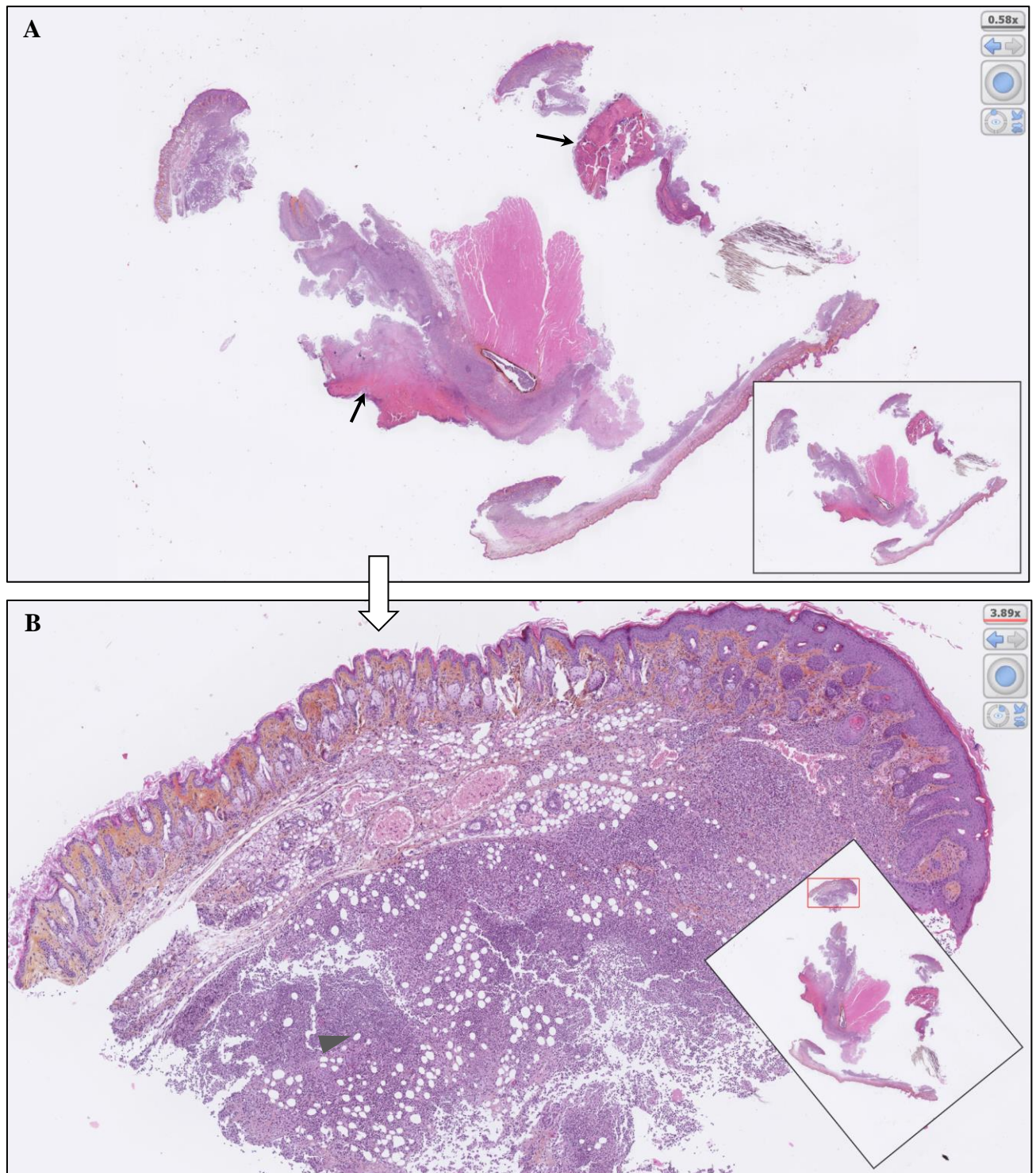


Figure S3: HES-stained high-resolution scans of skin sample collected from a mouse infected with *L. major* and nontreated. (A) represents a global view of the scan. Necrotic zones are indicated by black arrows. (B) represents a magnification of a skin zone with invasive inflammatory granuloma dissociating muscle fibers and the adipocytes (white oval and round shaped, gray arrow).

III.3. Mice treated by IL injections of AmB-DOC

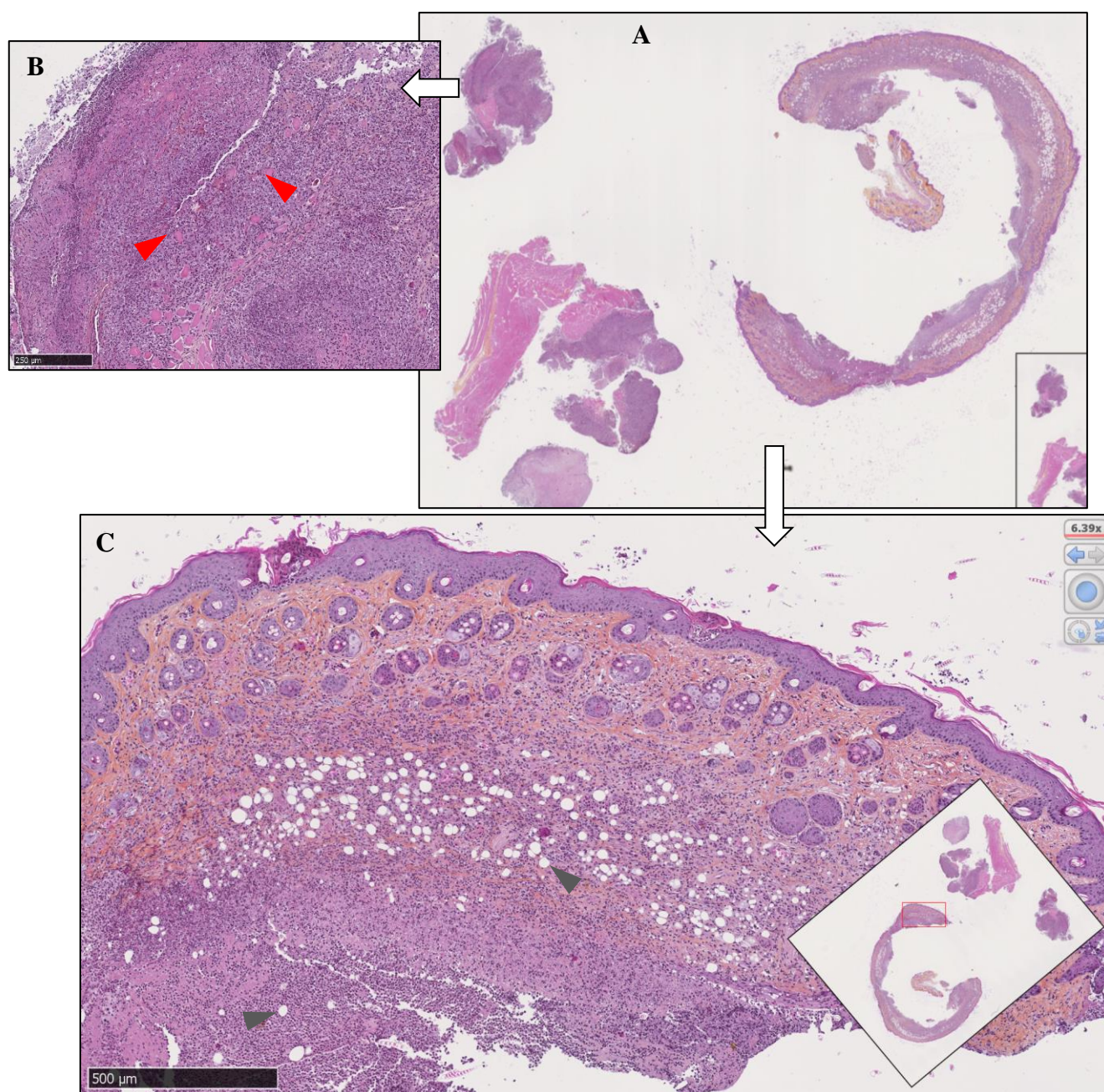


Figure S4: High-resolution scans of fragment of skin collected from a mouse infected with *L. major* and treated by IL injections of AmB-DOC after HES staining. (A) represents a full view of the scan. In (B) a magnification of a skin area with an invasive granuloma dissociating muscle fibers (stained pink, red arrows). In (C) the magnification showed a skin area with a granuloma dissociating the adipocytes (white oval and round shaped, gray arrows).

III.4. Mice treated by IL injections of Cs-NPs

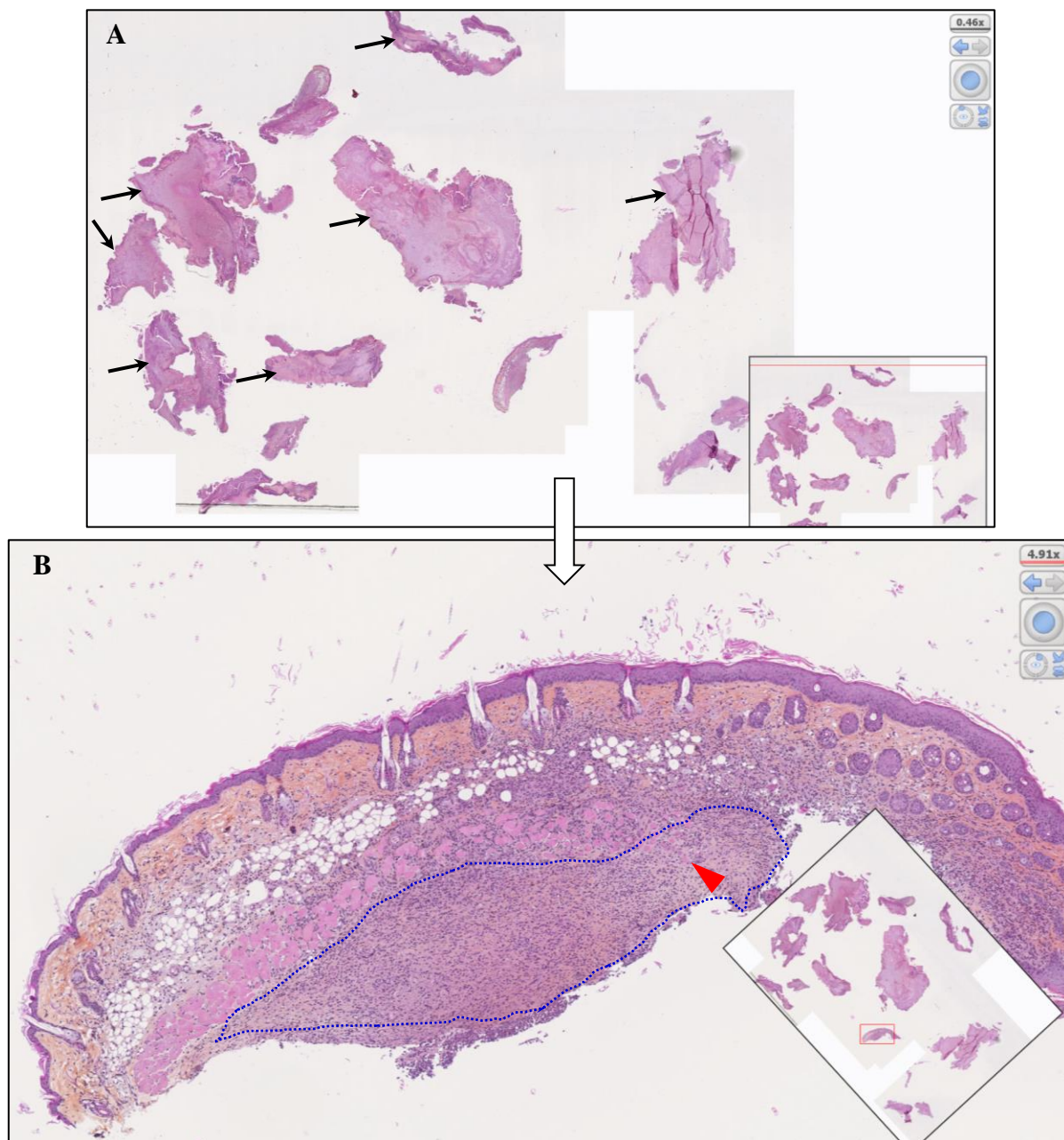


Figure S5: High-resolution scans of a skin fragment collected from of a mouse infected with *L. major* and treated by IL injections of Cs-NPs after HES staining. (A) represents a full view of the scan, where necrotic areas are indicated by black arrows. (B) In the magnification of a skin zone, deeply located granuloma is presented by blue dot line. Muscle dissociated with the granuloma is indicated by a red arrow.

III.5. Mice treated by IL injections of the combination of AmB-DOC and Cs-NPs

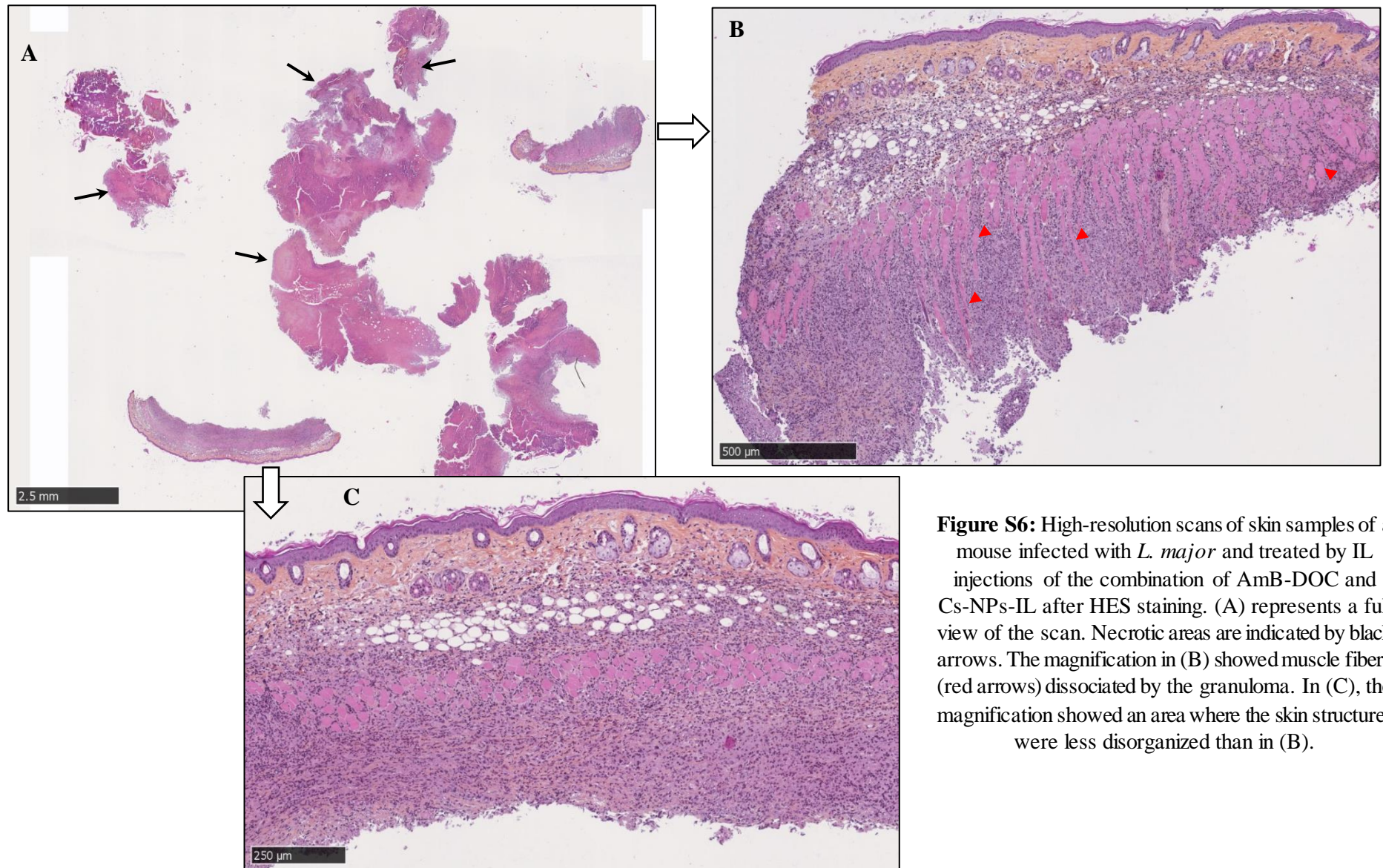


Figure S6: High-resolution scans of skin samples of a mouse infected with *L. major* and treated by IL injections of the combination of AmB-DOC and Cs-NPs-IL after HES staining. (A) represents a full view of the scan. Necrotic areas are indicated by black arrows. The magnification in (B) showed muscle fibers (red arrows) dissociated by the granuloma. In (C), the magnification showed an area where the skin structures were less disorganized than in (B).

III.6. Mice treated with topical application of F127 hydrogel

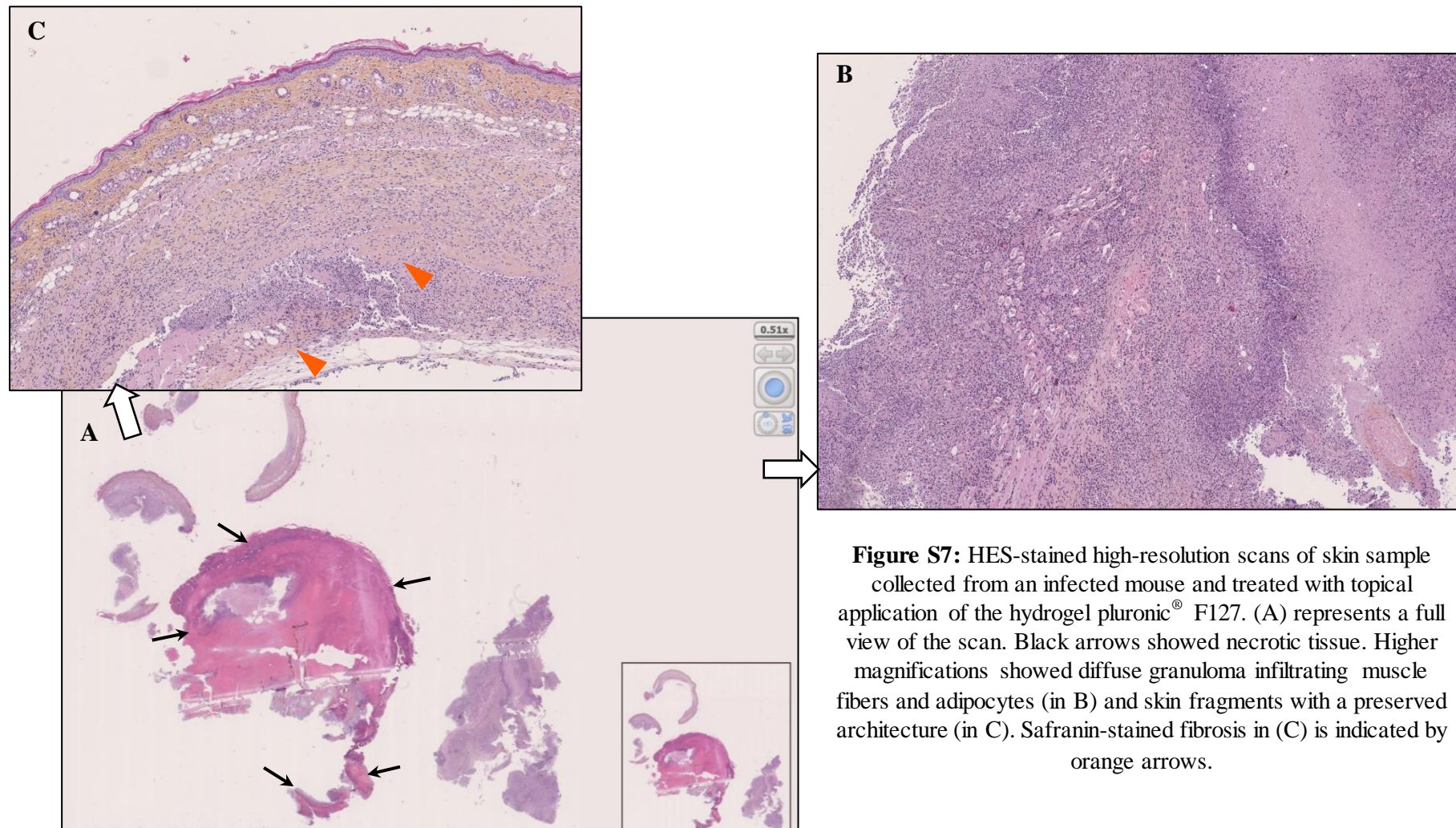


Figure S7: HES-stained high-resolution scans of skin sample collected from an infected mouse and treated with topical application of the hydrogel pluronic® F127. (A) represents a full view of the scan. Black arrows showed necrotic tissue. Higher magnifications showed diffuse granuloma infiltrating muscle fibers and adipocytes (in B) and skin fragments with a preserved architecture (in C). Safranin-stained fibrosis in (C) is indicated by orange arrows.

III.7. Mice treated topically with AmB-DOC_{F127}

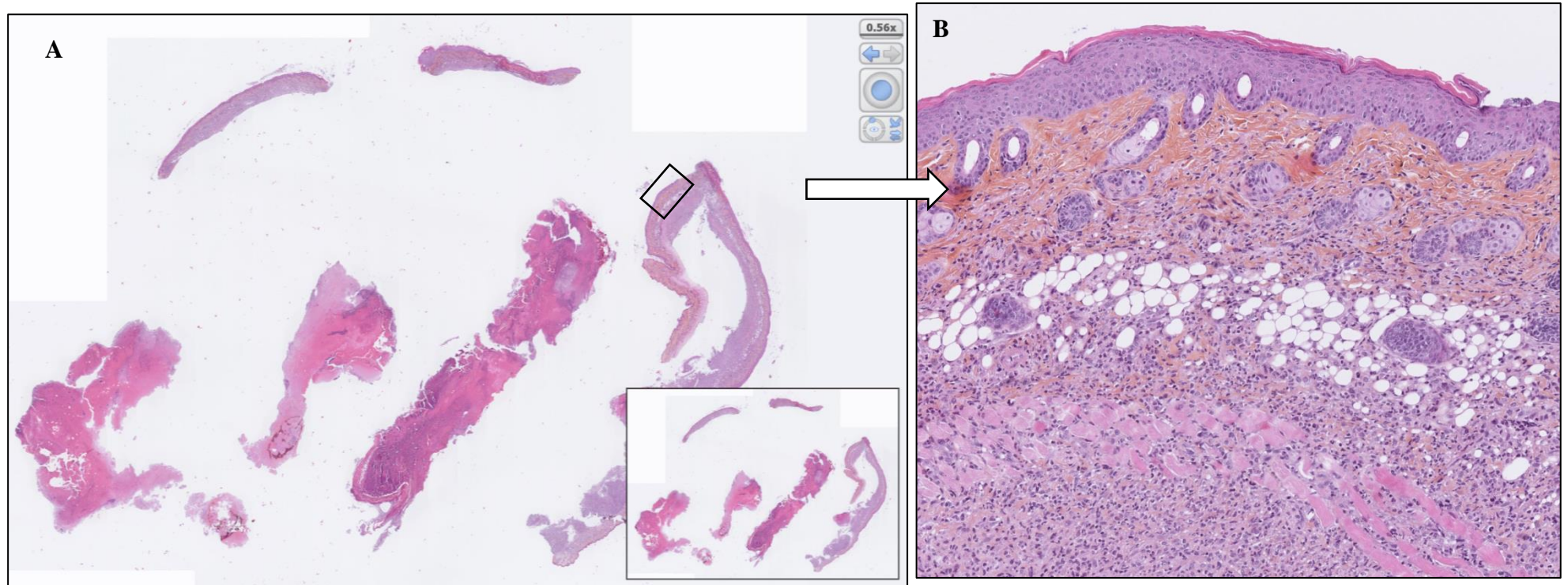


Figure S8: HES-stained high-resolution scans of skin sample collected from a mouse infected with *L. major* and treated topically with AmB-DOC_{F127}. (A) represents a full view of the scan. (B) represents a magnification of a zone showing a deep and invasive granuloma partly dissociating the muscle fibers and the hypodermis.

III.8. Mice treated topically with Cs-NPs_{F127}

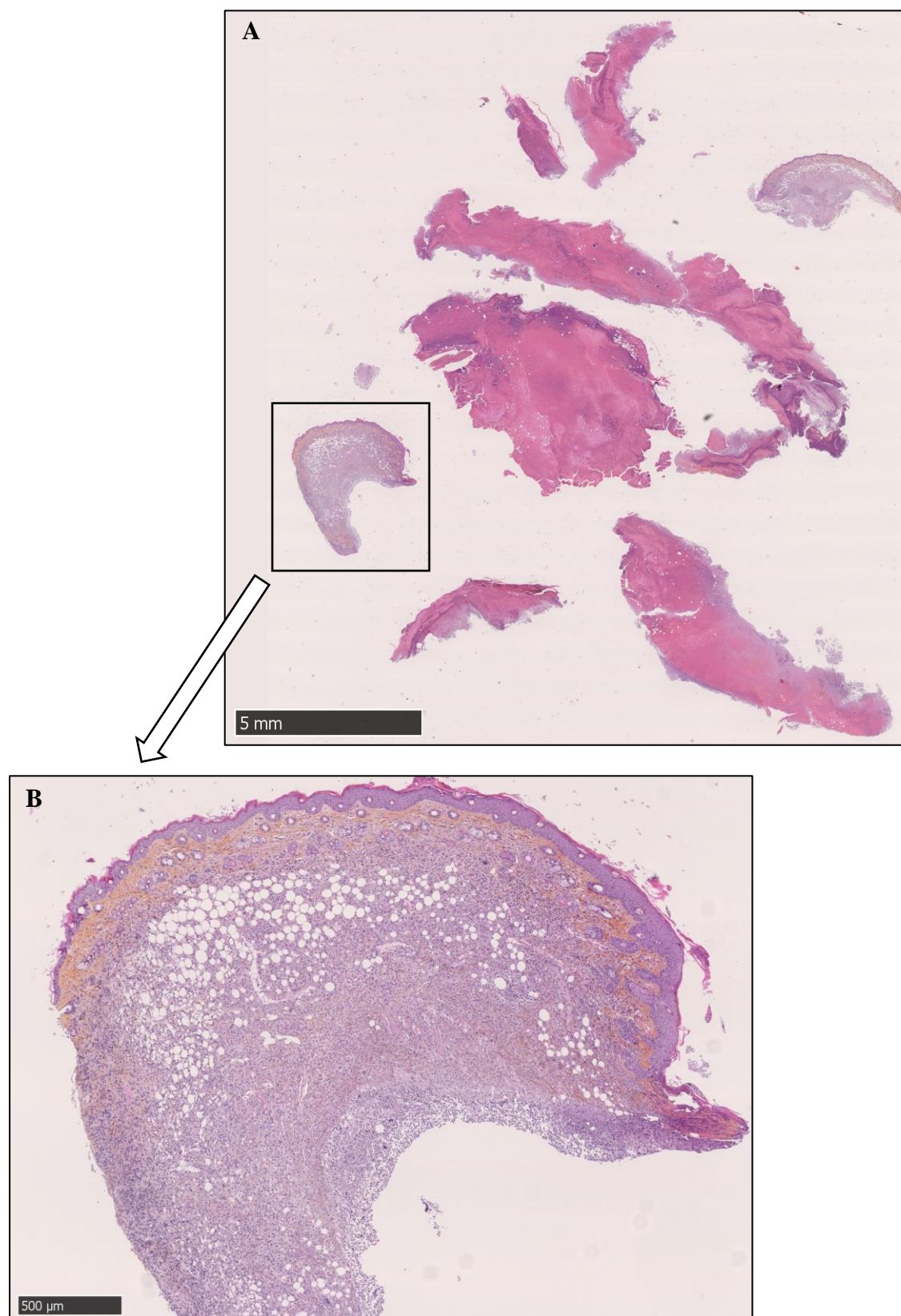


Figure S9: HES-stained high-resolution scans of skin sample collected from a mouse infected with *L. major* and treated topically with Cs-NPs/F127. (A) represents a full view of the scan. (B) represents a magnification of a skin infiltrated by the granuloma dissociating the hypodermis.

III.9. Mice treated with the combination (Cs-NPs/AmB-DOC)_{F127}

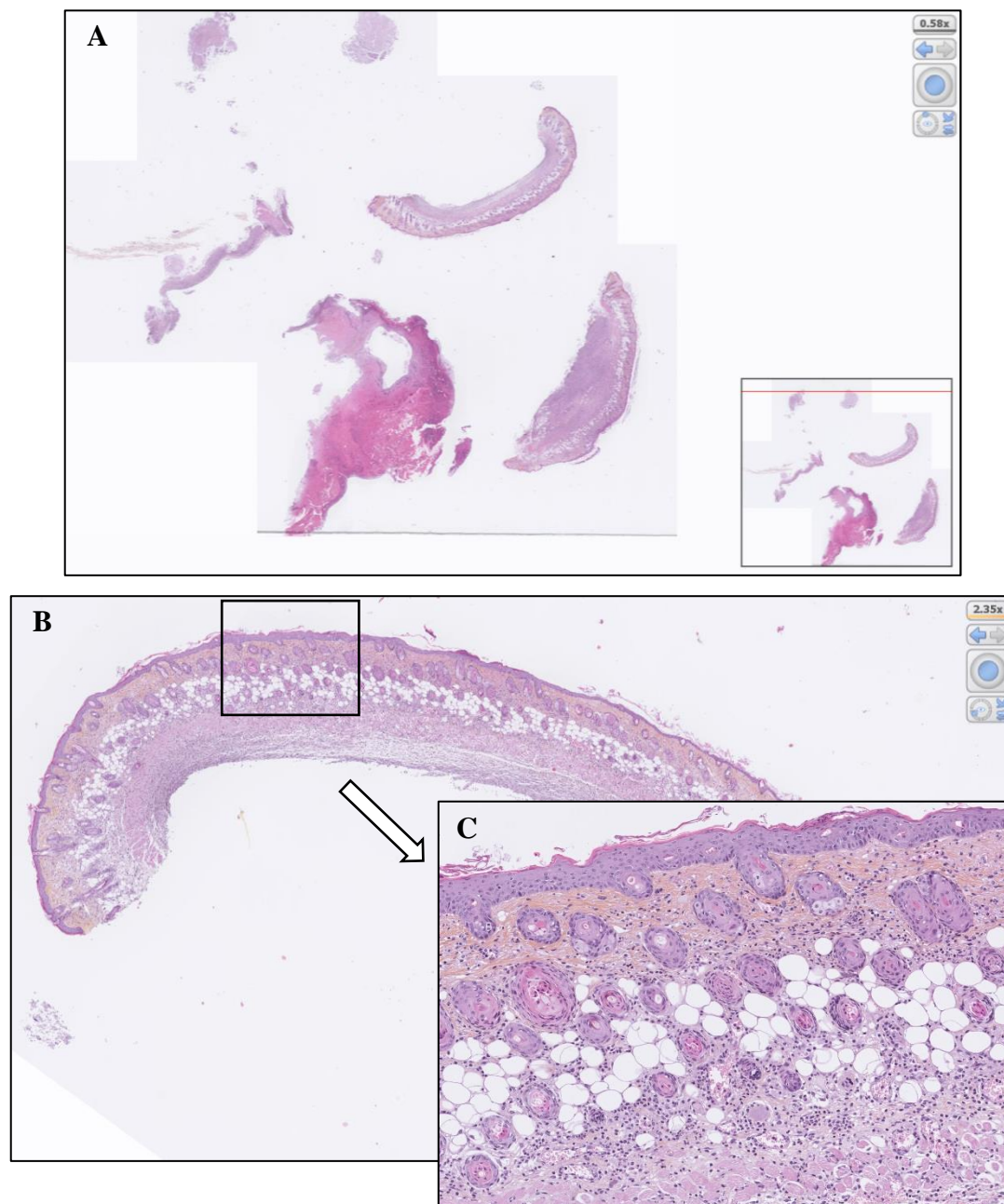


Figure S10: HES-stained high-resolution scans of skin sample collected from a mouse infected with *L. major* and treated topically with the combination (Cs-NPs/AmB-DOC)_{F127}. A full view of the scan is given in (A). (B) and (C) are two magnifications of a zone, where the skin architecture was preserved.

IV. Quantification of *L. major* genomes by q-PCR

IV.1. Genomic DNA preparation

Total DNA was isolated from formalin-fixed, paraffin-embedded (FFPE) skin biopsies using 4-8 sections (4 µm). Paraffin blocks without tissue sample served as negative and cross-contamination controls. Tissue from each section was collected by scraping-off the material from the block with a disposable sterile scalpel blade and incubated for 10 min at 95°C in 200 µL of TE buffer (50 mM Tris-HCl, pH 8; 1 mM EDTA). After 20-min centrifugation at 12,000 g at 4°C, the paraffin ring formed over the buffer was removed. After the addition of 300 µL of TE lysis buffer and 2.5 µL of proteinase K (20 mg/mL), the samples were incubated at 55°C overnight, followed by supplementary digestion with 5 µL of additional proteinase K (20 mg/mL) under agitation for 90 min at 55°C. After inactivation of proteinase K for 10 min at 95°C, the samples were vortexed and centrifuged for 10 min at 13,000 g. The supernatant was vortexed with one volume of phenol/chloroform/isoamyl alcohol (50/49/1) and centrifuged at 10,000 g for 5 min at room temperature. The supernatant was twice mixed with one volume of chloroform and centrifuged at 10,000 g for 5 min at room temperature. Next, DNA in the upper aqueous was precipitated by mixing with 1/25 volume of 5 M sodium chloride and 1 volume of isopropanol, followed by incubation for 30 min at -20°C. The pellet recovered after 10-min centrifugation at 10,000 g was rinsed with 70% ethanol, air dried for 30 min, dissolved in 50 µL TE buffer and solubilized by 10-min incubation at 55°C. Standard genomic DNA was similarly prepared from a 10-mL culture containing 10⁶ *L. major* parasites/mL.

IV.2. q-PCR analysis

The quality of DNA samples was first checked regarding the risk of false-negative results that could be due to DNA degradation and/or from the presence of PCR-inhibiting contaminants in the DNA extracts. The reproducibility of the amplification signal provided by ACTA1 mouse gene was thus checked in all samples. These q-PCR analyses were performed on 5 ng of total DNA using the SSoADV Univer SYBR[®] Green Supermix (Bio-Rad) reagent according to the manufacturer's instructions, with a 500-nM final concentration of each primer (forward: 5'-CGCTCTTGTGTGTGACAACG-3'; reverse: 5'-CCACGATGGATGGGAACACA-3') in duplicate 10-µL reactions comprising 45 two-step cycles (95°C 5 s; 60°C 30 s), in a CFX96(TM) real time thermal cycler (Bio-Rad). A previously described real-time PCR assay amplifying a short fragment of ribosomal RNA gene⁸ was used to detect *Leishmania*-specific DNA fragments (forward: 5'-AAGTGCTTTCCCATCGCAACT-3'; reverse: 5'-GACGCACTAAACCCCTCCAA-3'). Quantification of *L. major* genomes was performed using 5 ng of total DNA using the SYBR Green assay in 10-µL PCRs using the SSoADV Univer SYBR[®] Green Supermix (Bio-Rad) reagent according to the manufacturer's instructions, with 500-nM final concentrations of each primer, in triplicate 10-µL reactions, by 45 two-step cycles (95°C 5 s; 60°C 30 s). The results were confirmed by

the hydrolysis probe assay (FAM-5-CGGTTCGGTGTGTGGCGCC-3-TAMRA) using SSoFast Probes SuperMix (Bio-Rad), 500-nM final concentrations of each primer, 200 nM of probe and 5 ng of total DNA in duplicate 10- μ L reactions, by 45 two-step cycles (95°C 5 s; 60°C 30 s). The copy number of *L. major* genomes was measured from each skin sample against a standard curve generated from the standard *L. major* genomic DNA ranging from 10 to 10⁶ genomes per PCR. The PCR efficiencies calculated for each gene from the slopes of the calibration curves generated from a standard mouse or *L. major* DNA sample were above 95%.

IV.3. Results of the quantification of mice actin by q-PCR

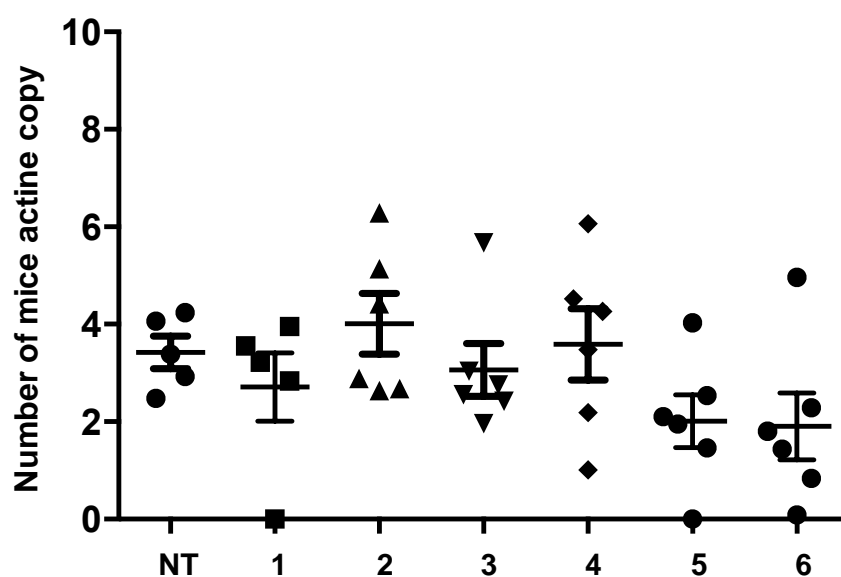


Figure S11: Quantification of mice actin copy in nontreated group (NT) and mice groups treated with F127 20 wt% hydrogel (1), AmB-DOC_{F127} (2), AmB-DOC_{IL} (3), Cs-NPs_{IL} (4), Cs-NPs_{F127} (5) and (Cs-NPs/AmB-DOC)_{F127} (6).

V. TEM observations

*V.1. Experimental method for the investigation of the *L. major* ultrastructure after incubation with Cs-NPs using TEM*

The method was adapted from our previous work.² After each incubation time, the cultures were washed twice with PBS to remove the culture medium and then were fixed with 2% glutaraldehyde in 0.1 M Na cacodylate buffer at pH 7.2 for 1 h at room temperature as reported in our previous work.² The samples were then contrasted with Oolong Tea Extract (OTE) 0.5% in cacodylate buffer, postfixed with 1% osmium tetroxide containing 1.5% potassium cyanoferrate, gradually dehydrated in ethanol (30% to 100%) and substituted gradually in the mix of ethanol-epon and embedded in Epon. (*Delta microscopie, France*). Thin sections (70 nm) were collected onto 200-mesh copper grids and counterstained with lead citrate. The grids were examined using a Hitachi HT7700 electron microscope operated at 80 kV (Elexience, France), and images were acquired with a charge-coupled device camera (AMT).

V.2. TEM image of control untreated sample



Figure S12: Representative image of cell body *L. major* promastigote specimen in a thin section observed by transmission electron microscopy. M: mitochondria, g: Golgi, V: multivesicular bodies. Scale bar: 1 μ m.

V.3. TEM image after 20-min incubation with Cs-NPs

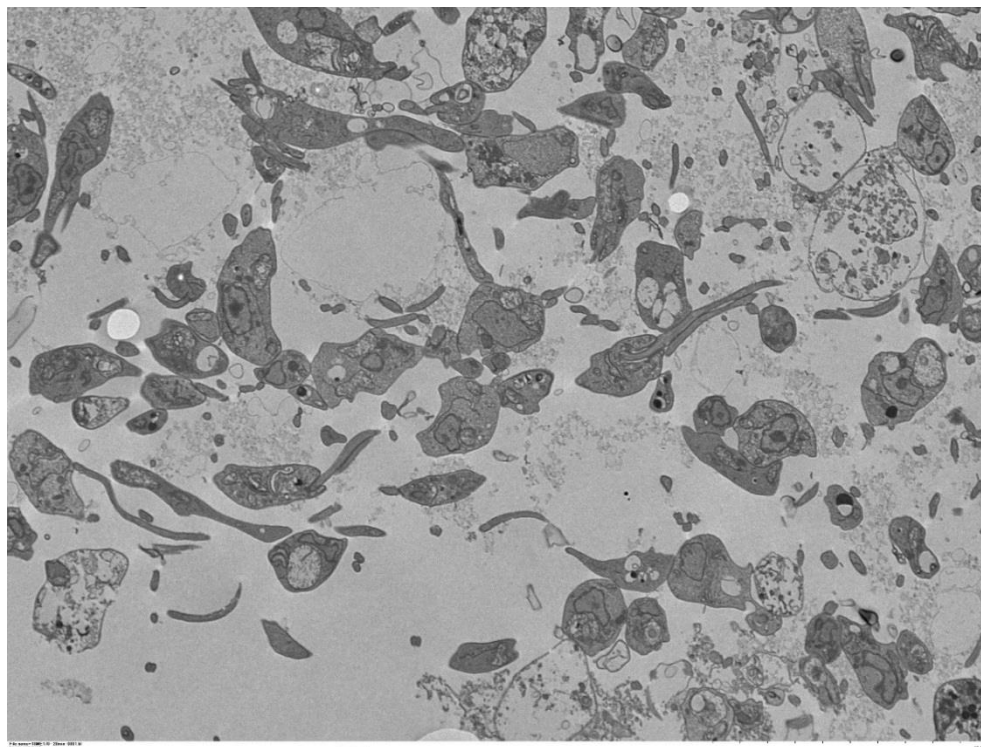


Figure S13: TEM image showing abnormal morphologies of *L. major* promastigotes after 20-min incubation with Cs-NPs.

V.4. TEM image after 1-h incubation with Cs-NPs

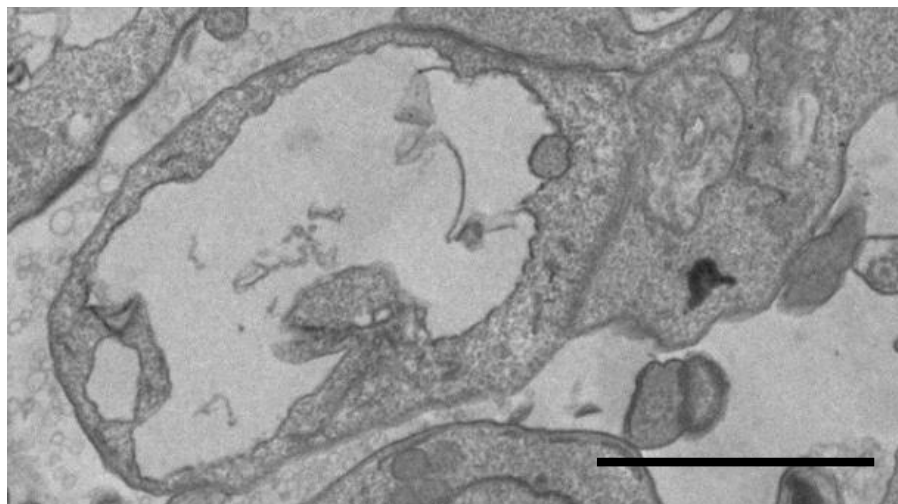


Figure S14: TEM image of *L. major* after 1-h incubation with Cs-NPs. Scale bar: 2 μ m. The image showed a specimen with aberrant shape and where internal structures were quasi-absent.

References

1. Pradines, B.; Bories, C.; Vauthier, C.; Ponchel, G.; Loiseau, P. M.; Bouchemal, K., Drug-free chitosan coated poly (isobutylcyanoacrylate) nanoparticles are active against *Trichomonas vaginalis* and non-toxic towards pig vaginal mucosa. *Pharmaceutical research* **2015**, 32 (4), 1229-1236.
2. Malli, S.; Bories, C.; Bourge, M.; Loiseau, P. M.; Bouchemal, K., Surface-dependent endocytosis of poly (isobutylcyanoacrylate) nanoparticles by *Trichomonas vaginalis*. *International journal of pharmaceutics* **2018**, 548 (1), 276-287.
3. Daligaux, P.; Pomel, S.; Leblanc, K.; Loiseau, P. M.; Cavé, C., Simple and efficient synthesis of 5'-aryl-5'-deoxyguanosine analogs by azide-alkyne click reaction and their antileishmanial activities. *Molecular diversity* **2016**, 20 (2), 507-519.
4. Malli, S.; Pomel, S.; Dennemont, I.; Loiseau, P. M.; Bouchemal, K., Combination of amphotericin B and chitosan platelets for the treatment of experimental cutaneous leishmaniasis: Histological and immunohistochemical examinations. *Journal of Drug Delivery Science and Technology* **2019**.
5. Balaraman, K.; Vieira, N. C.; Moussa, F.; Vacus, J.; Cojean, S.; Pomel, S.; Bories, C.; Figadère, B.; Kesavan, V.; Loiseau, P. M., In vitro and in vivo antileishmanial properties of a 2-n-propylquinoline hydroxypropyl β -cyclodextrin formulation and pharmacokinetics via intravenous route. *Biomedicine & Pharmacotherapy* **2015**, 76, 127-133.
6. Jagu, E.; Pomel, S.; Diez-Martinez, A.; Rascol, E.; Pethe, S.; Loiseau, P. M.; Labruère, R., Synthesis and antikinetoplastid evaluation of bis (benzyl) spermidine derivatives. *European journal of medicinal chemistry* **2018**, 150, 655-666.
7. Mao, W.; Daligaux, P.; Lazar, N.; Ha-Duong, T.; Cavé, C.; van Tilbeurgh, H.; Loiseau, P. M.; Pomel, S., Biochemical analysis of leishmanial and human GDP-Mannose Pyrophosphorylases and selection of inhibitors as new leads. *Scientific reports* **2017**, 7 (1), 751.
8. Gebhardt, M.; Ertas, B.; Falk, T.; Blödorn-Schlicht, N.; Metze, D.; Böer-Auer, A., Fast, sensitive and specific diagnosis of infections with *Leishmania* spp. in formalin-fixed, paraffin-embedded skin biopsies by cytochrome b polymerase chain reaction. *British Journal of Dermatology* **2015**, 173 (5), 1239-1249.